



## Sampling in precision agriculture: A software for navigation in field activities

Juliano Rodrigo Lamb<sup>a,b,\*</sup>, Everton Coimbra Araújo<sup>a</sup>, Claudio Leones Bazzi<sup>a</sup>, Márcio Furlan Maggi<sup>b</sup>

<sup>a</sup> Department of Computer Science, Federal University of Paraná (UTFPR), Medianeira, Paraná, Brazil

<sup>b</sup> PGEAGRI, Technological and Exact Sciences Center, Western Paraná State University (UNIOESTE), Cascavel, Paraná, Brazil



### ARTICLE INFO

#### Keywords:

Precision agriculture  
Android  
Smartphones  
Agriculture technology

### ABSTRACT

The use of mobile devices in agricultural activities (such as smartphones and tablets) is still incipient; however, they can be used in several field activities, such as land demarcation, data recording and sample point location in Precision Agriculture (PA) due to their processing capacity, mobility and integrated geolocation systems. In addition to their lower cost compared to commercial low-cost GNSS equipment used for this purpose, these devices present more attractive features and resources. This study aimed to develop an application for mobile devices to generate paths for the location of georeferenced sample points by importing data in text format. Two algorithms were evaluated to generate the walking paths (Greedy and Simulated Annealing) and a path generated by an expert. To ensure the accuracy of the results, the precision of a smartphone and a low-cost GNSS equipment were evaluated using an RTK station. The tests with the application proved the similarity of the smartphone with other commercial low-precision devices. The device accuracy can be used in data collection activities for PA, especially when working with Management Zones (Mzs) where precision is not a limiting factor because it is a method that aims to make PA concepts viable, even using machines and equipment from conventional agriculture.

### 1. Introduction

Several technologies are required to adopt Precision Agriculture (PA) in agricultural management, including productivity monitoring, global navigation satellite system (GNSS) technologies, mapping systems, and application at variable rate, among others. In this sense, focusing on soil and plant management and the use of different inputs (such as fertilizers, herbicides, seeds and fuel, among others) that are used in correct places and moments, PA technology seeks to increase crop productivity and reduce its production costs, in addition to reducing the effects caused by agriculture on the environment [1–3].

Spatial mapping and temporal variability of soil, plant, and climate attributes is an important part of PA. The variability in fields means a land should not be treated uniformly, but rather with techniques for inputs at variable rates, or maybe even divided into management zones (Mzs). The use of Mzs is a strategy for applying PA when farmers have only traditional machines and equipment available, not having variable rate application machines, harvest monitoring or advanced software

resources, for example. For these farmers, within each Mz, conventional machines and equipment are used, applying fixed rates and varying the management between zones with different productivity potentials [4]. This strategy is also a solution to adjust the relationship between the economic aspects and the benefits obtained with PA [5]. Mzs can also guide soil sampling, allowing composite samples to be taken for each subregion, given that soil fertility and texture characteristics tend to suffer little variation. This enables PA's viability from an economic point of view, with good results.

Thus, understanding spatial variability is necessary to implement different management techniques. Such in-the-field management depends on the attributes under study, which may vary over short or long distances (from meters to hundreds of meters) [4], [5]. The correct diagnosis of spatial variability of soil and crop properties varies according to several factors, such as soil type, biome, climate, and agricultural practice [6], widely varying in different regions [5].

The determination and mapping of spatial variability usually requires normally dense sampling—which implies operational difficulties

\* Correspondence to: Av. João XXIII, 2755, Medianeira, Paraná CEP: 85884-000, Brazil.

E-mail addresses: [lamb@utfpr.edu.br](mailto:lamb@utfpr.edu.br) (J.R. Lamb), [everton@utfpr.edu.br](mailto:everton@utfpr.edu.br) (E.C. Araújo), [bazzi@utfpr.edu.br](mailto:bazzi@utfpr.edu.br) (C.L. Bazzi), [marcio.maggi@unioeste.br](mailto:marcio.maggi@unioeste.br) (M.F. Maggi).

and high costs for data collection. Thus, sampling methods that enable the determination of spatial variability of attributes at lower costs is necessary. Sampling is an essential step of PA cycle, since it is virtually related to the quality and accuracy of determining the spatial variability of factors, enabling more precise decisions [4].

Given this context, several approaches promote the use of techniques that reduce the number of sampling points. These approaches have focused on statistical studies, such as [7] and [8]; on the use of remote sensing instead of conventional sampling [9] or even on the development of precise and low-cost GNSS solutions such as [10–12].

Mobile devices can be used to support data collection for mapping spatial variability. [13–15] point out the promising use of smartphones in agricultural processes due to their mobility, computational power, and variety of mobile applications (apps) available. [13] also state that the traditional technology already contributes significantly to communication, enabling agricultural farmers to access accurate and timely information on inputs and market, even in the field.

[14] identified 22 studies on the use of mobile devices in agricultural operations, mostly focused on property management. A review by [16] identified 38 studies in this area, four of which developed mobile applications for field mapping and soil information, as follows:

1. AGRI PRECISION: presented by [17], this application uses the GNSS sensors of the mobile device to generate sampling points and grids. It allows delimiting the contour of the field and point to point navigation, not recording the browsing history. It does not require an internet connection and does not allow the import of sample points from other pieces of software;
2. GPS FIELDS AREA MEASURE: presented in [18,19], it uses the GNSS sensors of the mobile device, recommending the use of an external antenna to improve accuracy. It does not require an internet connection. This mobile application is focused on the measurement of field, area, and perimeter, also enabling the highlighting of points of interest;
3. SOIL SAMPLER: available in the online app store for Android [20], this application is similar to Agri Precision. It allows for the demarcation of lines, selection of the number of sample points for generation of sampling grids, with navigation between them. Internet connection is required. It does not present information about the process of route generation and does not allow the import of sample points from other pieces of software;
4. NITROGEN INDEX: described by [21], it is a specific mobile application to estimate nitrogen content in a soil. It uses the cellphone GNSS sensors and does not require internet connection.

The number of publications and their scope has evolved, according to the studies by [14,16]. The later also points the existence of software packages without scientific basis in app stores (i.e.: Google Play or App Store). Some apps present low-rated reviews among users, are paid or not available in English, thus being excluded from their review.

The four apps presented do not allow sample points to be imported from other pieces of software and lack information about the routes. Moreover, information on the determination of navigation paths is absent. These factors imply the disregarding of a very significant element in the process of agricultural management: user experience, as stressed by [22].

The lack of applications with these features represents a gap that, when filled, can innovate and contribute to the popularization of PA, especially when using low-cost devices. The presence of a GNSS sensor on mobile devices and the development of PA applications is innovative, providing an alternative to current sampling methods, transforming some user habits and providing new features and advantages that make the process more efficient and simplified. The study of this area revealed yet another problem, which is precisely the lack of information about the accuracy of this type of device [23], information that may or may not limit their use in sampling activities [4] or MZ delineation, for example.

From a practical point of view, numerous soil sample collection activities do not require millimeter precision in the context of PA, considering that the variation between these collected attributes is perceptible by geostatistics (semivariogram) from several meters or tens of meters, obtained by the special dependence between samples. For PA to become more popular, it is important that digital resources and applications can enable the use of PA techniques, even for small farmers, who cannot make large investments in the area. For farmers who work with MZs, these less accurate and cheaper resources are interesting so that they can work and make the PA viable to improve their productivity and increase their profits with low investment.

In addition to the study related to geolocation devices, the evaluation of walking routes is also relevant because, by applying different algorithms, routes that may result in shorter distances to be covered can be generated; this problem is similar to the study of [24].

Given this context, this study aimed to (i) assess the precision of a smartphone and of a low-cost GNSS device in the location of known sampling points to identify whether such devices can be used in PA, especially when working with MZs; and (ii) present an app developed to assist farmers and service providers in the management of georeferenced sampling points and enable them to guide their location to the field assisted by optimized routing techniques based on resources available for mobile devices.

## 2. Materials and methods

### 2.1. Defining system features

According to the system overview (Chart 1), software development should meet six main requirements.

After the requirements gathering analysis, six functional requirements (Table 1) that describe the main features of the app were defined. These features do not require internet connection; however, the mobile device must have a GNSS sensor.

The requirements were implemented – based on good practices of software development – as in the class organization showed in Fig. 1, with the presence of the interface ListProperties. There are three classes implementing this interface ListPropertiesFromDatabase, ListPropertiesFromNetwork, and ListPropertiesFromFile. These three implementations are related to the way properties can be retrieved and listed in the app initial software wizard. The wizard does not have direct access to any of the implementations, only with the abstract type, demonstrating the system flexibility and independence of concrete implementations.

Considered as the main one, the functional requirement F4 enables the user to navigate the field, presenting information on the route executed until a given moment and the remaining route. As the user moves in the area, a line is plotted on the app map representing the route executed. Another line represents the route suggested by the application serving as field guide.

This requirement has been implemented in such a way to define a logic common to modules where some type of navigation is performed. Regarding design, this is reflected in the organization of the classes, as in the diagram showed in Fig. 2. The abstract Navigator superclass contains the main methods and behaviors that should be common to all classes. The other classes inherit these behaviors in their creation.

The different classes that extend the Navigator superclass (Fig. 2) include the implementations provided in the pathway planner, described by functional requirement F4. Functionally, in case of a subclass finding a target point, it will invoke an action according to the functionality currently running. If it is retrieving an observation point, an interface for control information (feedback) is displayed at that point. If the app is in a sampling activity, the user must register the attribute information that is being monitored in that collection activity, according to functional requirement F5. In sampling, after recording the value of the obtained attributes for a certain point, the system automatically

System for navigation in field activities – SNAC	
<p>Navigation software should improve the process of locating sampling points in the field during sampling activities where accuracy is not critical. Thus, it is expected to replace the use of conventional GNSS receivers and optimize the <b>orientation</b> with the definition of routes, metrics such as the shortest distance to go across the sample points predicted in a previously created sampling grid. The determination procedure of the shortest distance should not consider ground relief or obstacles, slopes or depressions. The app should also enable the registration of lands and their respective collection points. It should allow starting the navigation by selecting the lands already registered, allowing users to choose any starting point or start from locations suggested by the application. When determining the starting point, the system should trace routes, show the distances for each next point and indicate the route that would reach all sampling points. The system should also record the occurrences of weeds and pests, i.e., enabling the georeferencing of the location of such occurrence in the field. The use of this app should enable sampling even without using conventional GNSS, besides reducing the time spent on walking during the activity.</p>	

Chart 1. System Overview.

**Table 1**  
Main functional requirements of the app.

Identifier	Requirement: Description
F1	<b>Property management:</b> The system should allow the registration of properties in which sampling activities are conducted.
F2	<b>Attribute management:</b> The system should allow the registration of attributes that can be measured during sampling.
F3	<b>Observation point management:</b> The system should allow the registration of places of the user's interest.
F4	<b>Route planning:</b> The system should plan the walking path from the user's current location to an established endpoint.
F5	<b>Point location:</b> When a point is located, an action must be performed, depending on the functionality of the app running.
F6	<b>Starting point selection:</b> The system should allow the selection of the starting point in sampling activities.

changes the target point to the next sampling point, according to its predefined path.

The pathway planner also involves determining routes. When determining the route from user location to any point, the route consists of a line with starting and ending points in the coordinates involved. However, in sampling activities in which multiple points must be observed, a route can be determined in different ways, and there is no solution considered optimal. This route must go from the origin to the destination, passing through all intermediary points. This problem is known in the literature as a travelling salesman problem, as described by [25], and there are many approaches to its resolution. These approaches should balance the runtime by defining the shortest route, presenting no single optimal solution. In this context, the "Greedy" and "Simulated Annealing" algorithms are applicable [26,27].

The Greedy algorithm (G) uses the available information to seek an optimal solution at each stage to find a great global [28]. This algorithm is also known as the nearest neighbor algorithm, being one of the first approaches in computer science to determine a solution to the traveling salesman problem and with applications in the context of routing communication networks. Thus, one can determine a starting point for the algorithm to find the route. The shortest distances (greedy algorithm) are always considered as follows: based on the starting point "A," the algorithm finds the nearest point "B." From "B," the set of points (excluding point "A" already visited) is evaluated and the closest is found, and this approach is repeated until the completion of all points (**Algorithm 1**).

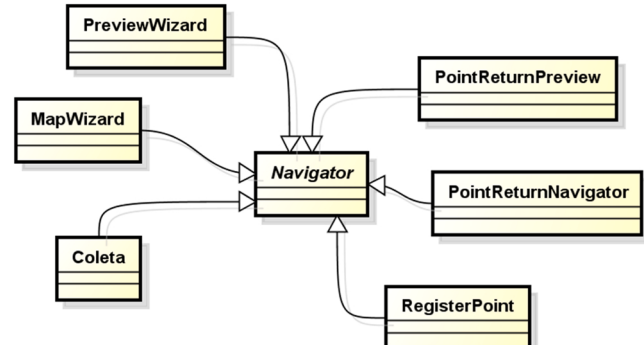


Fig. 2. Partial class diagram presenting the class hierarchy based on Navigator.

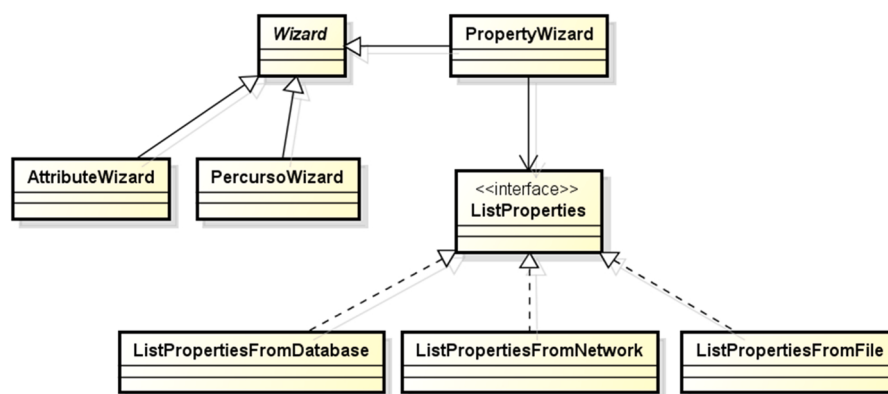


Fig. 1. Partial class diagram representing the dependency of abstract types.

**Algorithm 1.** A pseudocode for Greedy algorithm..

- 
1. Start the route from a single sampling point chosen by the user.
  2. Find the sampling point k outside the current route via the edge that ties it to the current point on the shortest distance.
  3. Add sampling point k to the final list of points visited.
  4. If all points were added, stop; if not, return to step 2.
- 

**Source:** [29]

The strategy of seeking the local optimal solution aiming at an optimal path (global optimal) is illustrated in Fig. 3, a representation of the displacement between points “A” and “J”. From point “A” the algorithm evaluates what is the shortest distance: until B (4 distance units – du) or C (3 du). The path to point “C” is chosen, as it is shorter, and represented by an orange line segment in this graph. The same decision is verified at each point, up to the destination, for a 27 du route. The graph in Fig. 3 also illustrates the algorithm’s limitation, since it cannot always identify the path with the shortest total distance (optimal path), represented by small red line segments, which totals 12 du.

The Simulated Annealing (SA) algorithm is related to optimization problems, especially in metallurgy [31,32], and the implementation proposed by [33]. Considering that, in metallurgy, a material must be heated at a very high temperature and then cooled down, the efficiency of this algorithm is directly linked to two internal variables: temperature and cooling rate [34]. A representation of its operation can be seen in the flowchart in Fig. 4.

This metaphor is applied in the algorithm, in which each cooling session iterations are performed in the search for solutions (**Algorithm 2**) [36]. Thus, the algorithm can identify a point as the beginning and determine a sequence to be traveled until full resolution of the set of points.

**Algorithm 2.** A pseudocode for Simulated Annealing algorithm..

- 
1. Set the initial temperature and create a random initial solution;
  2. Begin looping until the stop condition is met. Usually, either the system has sufficiently cooled, or a good-enough solution has been found;
  3. From here, it must be select a neighbor by making a small change to the current solution;
  4. Then, decide whether to move to that neighbor solution;
  5. Finally, decrease the temperature and continue looping.
- 

**Source:** [33]

The default route (P) adopted by the application is in the navigation of the points as arranged in the XML file. The system identifies the first point, adopts it as origin and goes through the other in sequence. This mechanism allows users to customize a route based on their own knowledge on an expert’s. This knowledge can be extremely significant in defining a route that considers field elevation, contour lines and other elements, especially in smaller or family farming areas.

The algorithms described above (G and SA) are classical and present methods in computing areas, especially related to optimization problems and adapted for such. The computational implementations of these differ since they derive from concepts and must be improved due to the restrictions present in computational languages. The default route (P), on the other hand, is not obtained by means of any algorithm but by an expert based on his knowledge of the area, usually provided by site visits.

The 3 methods described above (G, SA and P) can be used to determine routes and their use depends on the sampling scenario:

- a. If a pre-determined route created by an expert (P) exists, its use is recommended since it may account for elements such as field elevation and obstacles. However, a walking path created by the greedy algorithm (G) can be generated to then compare the final distance values of both;
- b. If no information on routes is available, route P cannot be used. Algorithms SA or G should then be used. While SA determines a route using a random starting point, G determines a route from a starting point chosen by the user. This option is interesting to select a point near the ends of each crop.

When it comes to coding in the app, this process is simplified for users: they do not pick the algorithm by name, they choose if they want a starting point or not. When the user selects a starting point, the Greedy algorithm is used to determine the route. If the option “random generation” is selected, Simulated Annealing is used.

The system architecture was elaborated according to the suggestions of the official documentation,<sup>1</sup> in which the necessary understanding of the language is available to access the hardware resources of mobile devices such as GNSS sensors and camera. These resources are used for registering user’s location and capturing images from observation

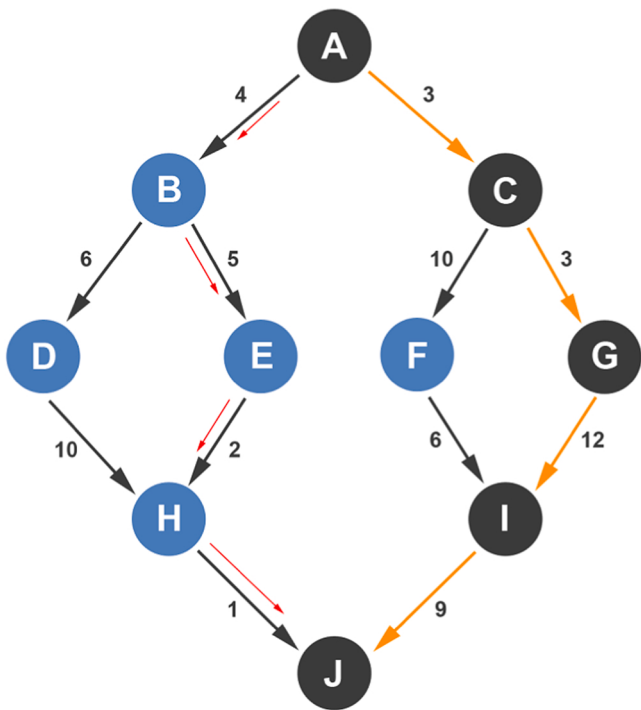
points, respectively.

## 2.2. Technologies used for software development

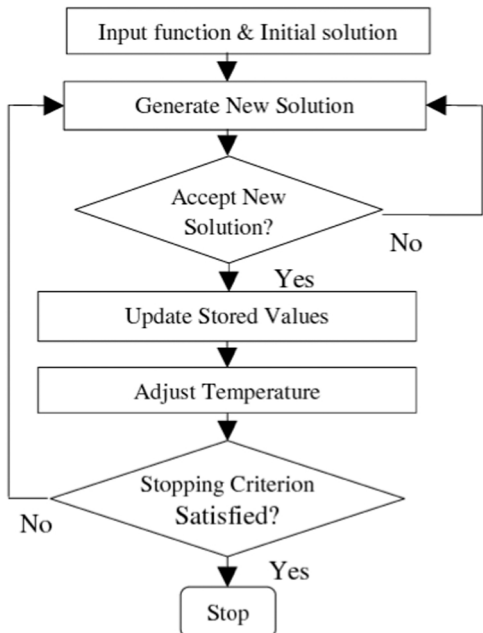
Considering that this app was designed for mobile devices (tablets and smartphones), with Android operating system (OS), free of license payment [37], we sought to work with open-source tools, enabling its free of charge availability to farmers, researchers, and service providers. The choice for the Android platform was also motivated due to the extensive documentation and technologies available for development support. Furthermore, the devices that support this OS are more accessible, i.e., they are cheaper when compared with other OS in market. The app was compiled to Android 9.0 (minSdkVersion = 19 and targetSdkVersion = 28).

Java [38] language was used in the Android Studio Integrated

<sup>1</sup> Available in <https://developer.android.com/>

**Fig. 3.** Greedy algorithm illustration.

Source: [30]

**Fig. 4.** Flowchart of the simulated annealing algorithm working.

Source: [35]

Development Environment [39] with the Google API [40]. The data persistence structure was built using the SQLite database system [41], all of which are free. The administration of software versioning in the development and coding stages of the project used the GitHub server [42].

Good programming practices were used during app development, such as Object-Oriented Programming (OOP), Design Principles and Design Patterns, as suggested by [43]. These techniques allow for the

development of classes and objects, or even components – allowing future addition of new modules, with minimal effect on the coding performed in previous versions.

### 2.3. Software validation procedures

The first step to validate the software was to check if behavior of a smartphone could be considered similar to that of a low-cost GNSS device in the location of known points. This test was conducted on experimental area A (Fig. 5).

Therefore, two devices were used to evaluate the dispersion and accuracy in the location of points: a smartphone (Equipment E1) Samsung Galaxy S10 + with multi-constellation GNSS receiver and Android 10; and a GNSS receiver (Equipment E2) Trimble Juno 3B with reception capacity for 12 parallel channels and tracking the C/A code on the Carrier L1, according to the manufacturer's specifications. The smartphone was randomly chosen, whereas the Juno receiver was chosen for being a commercially available equipment for this purpose, that is, demarcation of areas and location of points; and for being used in publications on Precision Agriculture, such as [44–47].

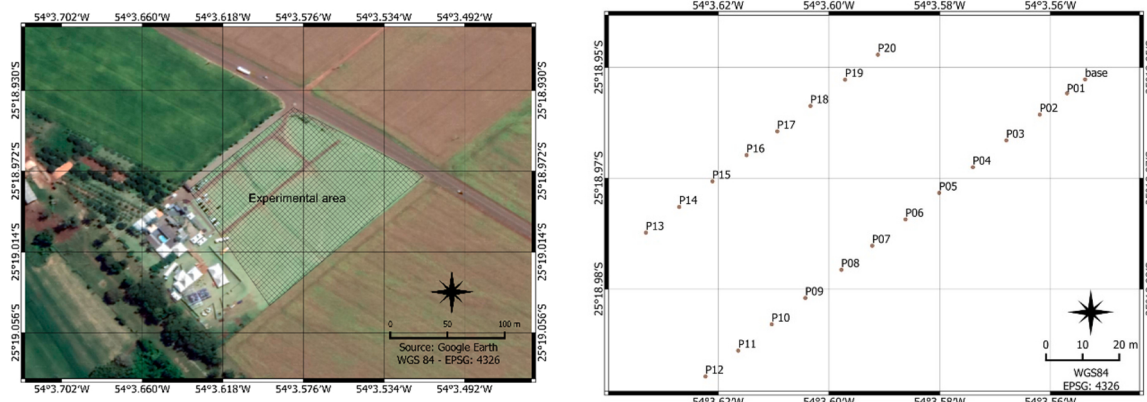
The dispersion of both devices was evaluated by a GNSS Trimble RTK R4 station, with the following accuracy values: 3 mm + 0.1 ppm RMS horizontally and 3.5 mm + 0.4 ppm RMS vertically, according to the manufacturer's specification. The station was built in a geodesic mark determined according to INCRA's technical standards and in compliance with Brazilian law 10267/2001. This mark is identified as 'base' on Fig. 5.

The georeferencing of 20 picket fences was performed with the RTK station in experimental area A (Fig. 5), located in the municipality of Medianeira/PR, under the coordinates 25°18'58.4"S 54°03'35.8"W. This area is approximately 2 ha in size and comprises an open field, without buildings or improvements, that is, the characteristics of an agricultural area. The spacing between picket fences used during the test to locate the points is approximately 10 m.

After georeferencing the picket fences and obtaining their coordinates, the coordinates were exported and loaded on the E1 and E2 equipment. The devices were then evaluated for their accuracy in the location of the picket fences. Equipment E1 used the SNAC software in the location, whereas the E2 device used the TerraSync software for navigation. The GNSS station was used to measure the error in the position given as correct by the equipment compared to the picket. Four repetitions were performed for each equipment, totaling 80 readings per device. The results were evaluated using dispersion graphs and descriptive statistics.

After testing the behavior of a mobile device in the retrieval of known points, the software was evaluated for route generation in an area that has been working with PA technology for at least 5 years (area B). The practical evaluation regarding the path among points generated by different routes was assessed in the determination of the sampling route in a rural property, located in the municipality of Céu Azul/PR, with about 15.5 ha in size (Fig. 6). With geometric center at coordinates – 53.832° E; – 25.109° N (WGS 1984) and 660 m in average altitude, the place is a commercial agricultural area cultivated under no-tillage system for over 15 years, with a succession of crops (soybean, corn and wheat). In this area, 40 sampling points are used to manage the spatial variability of soil attributes, with  $2.56 \text{ points ha}^{-1}$  in approximate density.

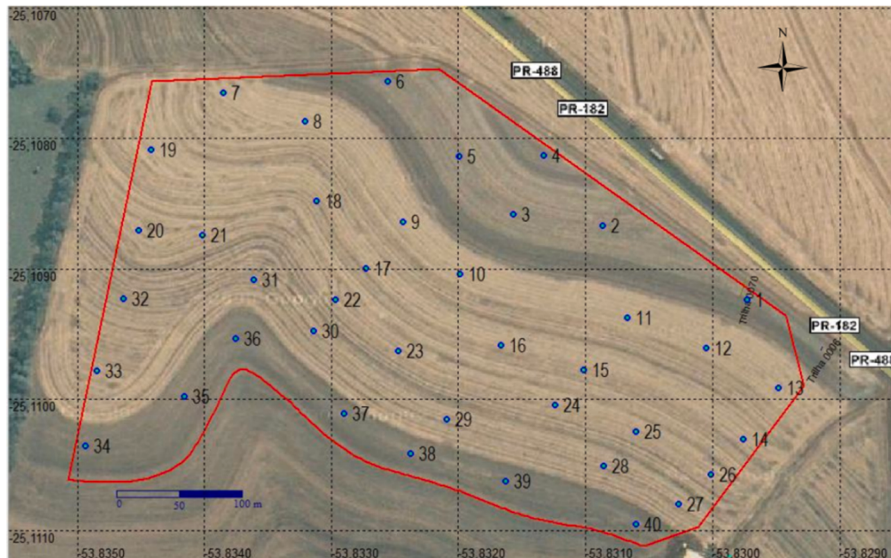
The evaluation of the algorithms used in the route elaboration was performed by observing their particularities. The method used in the determination of pathway P is based on an expert's knowledge and cannot be reproduced in the creation of routes with other starting points. The G algorithm traces a single route for each starting point – corresponding to the best solution. Then, 40 routes were determined for area B. The SA algorithm finds solutions using a variable called "cooling rate" (CR). Regarding this variable, the smaller its value, the higher the algorithm's ability to find an optimal solution at the cost of more



(a) Identification of the experimental area

(b) Location of picket fences

Fig. 5. Map of experimental area A, based on Google Earth images.

Fig. 6. Map of experimental area B, with sampling points identified.  
Source: [48].

processing capacity.

Pathway P was then evaluated, with the paths generated by G and SA algorithms by descriptive statistics, considering point 1 as the beginning and the default value for cooling rate (0.003), proposed in the [33] algorithm.

The mean values of pathway obtained by the G algorithm were evaluated with the SA algorithm and seven cooling rates per starting point. Considering that the SA algorithm does not allow the selection of a starting point, several runs were performed for each CR to achieve at least one execution per starting point. When more than one path was traced, the shortest one was considered.

The mean results obtained for each CR were subjected to a paired T-test to identify a better value for CR, so that the execution of the SA algorithm traces paths statistically lower than the G algorithm, on average.

The execution time for each route was measured since customized cooling rate implies an increased processing time.

### 3. Results and discussion

#### 3.1. Software presentation and major interfaces

The app finalized and named SNAC — System for Navigation in Field Activities (*Sistema para Navegação em Atividades de Campo*) (Fig. 7) is the product of the development phases.

The Fig. 7 shows the home screen, with six feature options, in compliance with the mentioned requirements:

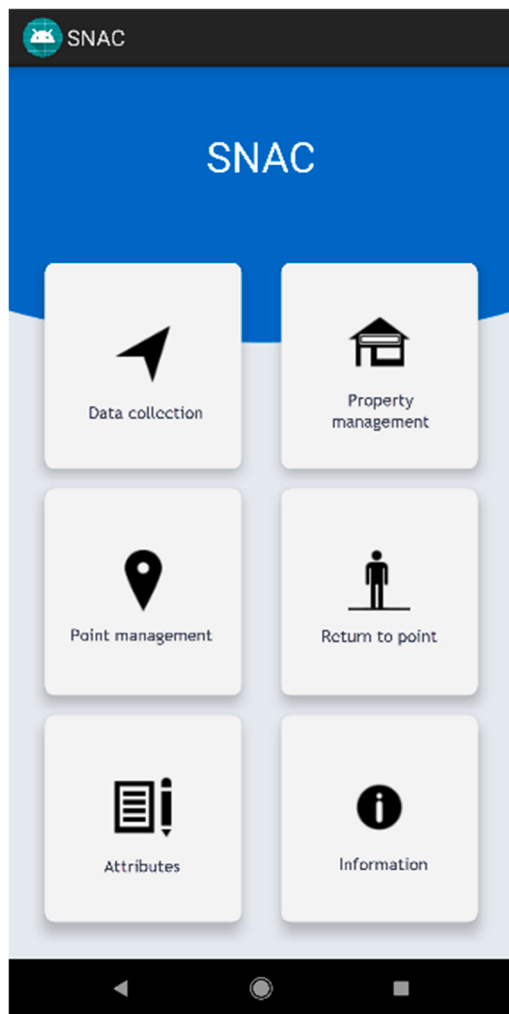


**Fig. 7.** SNAC Home Screen.

- Data collection: to perform sampling activities or visualization of existing records (shared requirement F4). [Fig. 8](#) describes the steps to be taken until the sampling activity begins;
- Property management: module related to the management of the field (according to functional requirement F1);
- Point management: module for management of observation point (according to functional requirement F3). [Fig. 8](#) describes the steps required until the operation is concluded;
- Return to point: navigation module similar to sampling, and in this image it is located only one observation point (shared requirement F4). [Fig. 8](#) describes the steps required until the operation is concluded;
- Attribute: module for management of the sampled attributes (according to functional requirement F2); and
- Information: corresponding to contact and system information.

The options presented on the initial screen ([Fig. 7](#)) provide quick access to the “Return to point,” “Point management” and “Data collection” options. These modules make use of information previously fed into the “Property management” and “Attribute” modules. The flowchart in [Fig. 8](#) enables a better understanding of these functionalities by describing the steps in each of the options in which the user interacts.

The module DATA COLLECTION for recording the observation point is simulated in [Fig. 9a](#). The system records the point based on the user’s location, who must fill in the information related to the phenomenon under observation, such as details and type of observation.

“Returning to an observation point” uses the navigation module, as shown in [Fig. 9b](#) and c. The observation point is presented with red marker and the user’s position with blue marker. The line segment in red corresponds to the route until the point location. The distance pane in the upper-left corner is updated as the user moves across the map.

The navigation module during sampling activities shares many elements of the interface previously presented in [Fig. 9](#), which can be seen in [Fig. 10](#). The map shown corresponds to walking in area A during precision and accuracy check tests.

[Fig. 10a](#) presents the navigation module; the red markers are the sampling points and the starting point is green. The user’s current position is represented by a blue mark and the route taken in red. A pane in the upper left corner displays information on the next point and the distances involved.

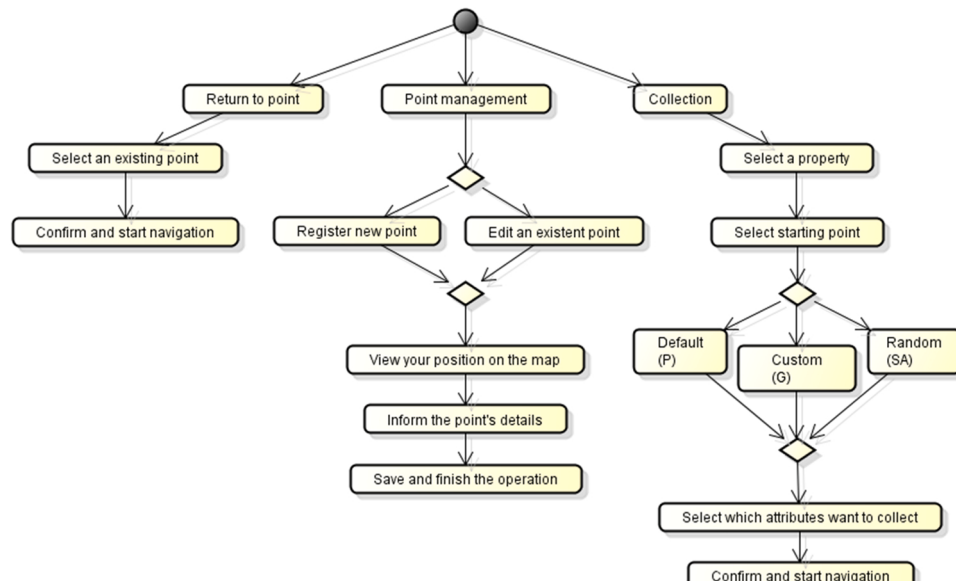


**Fig. 8.** Flowchart of the main features.

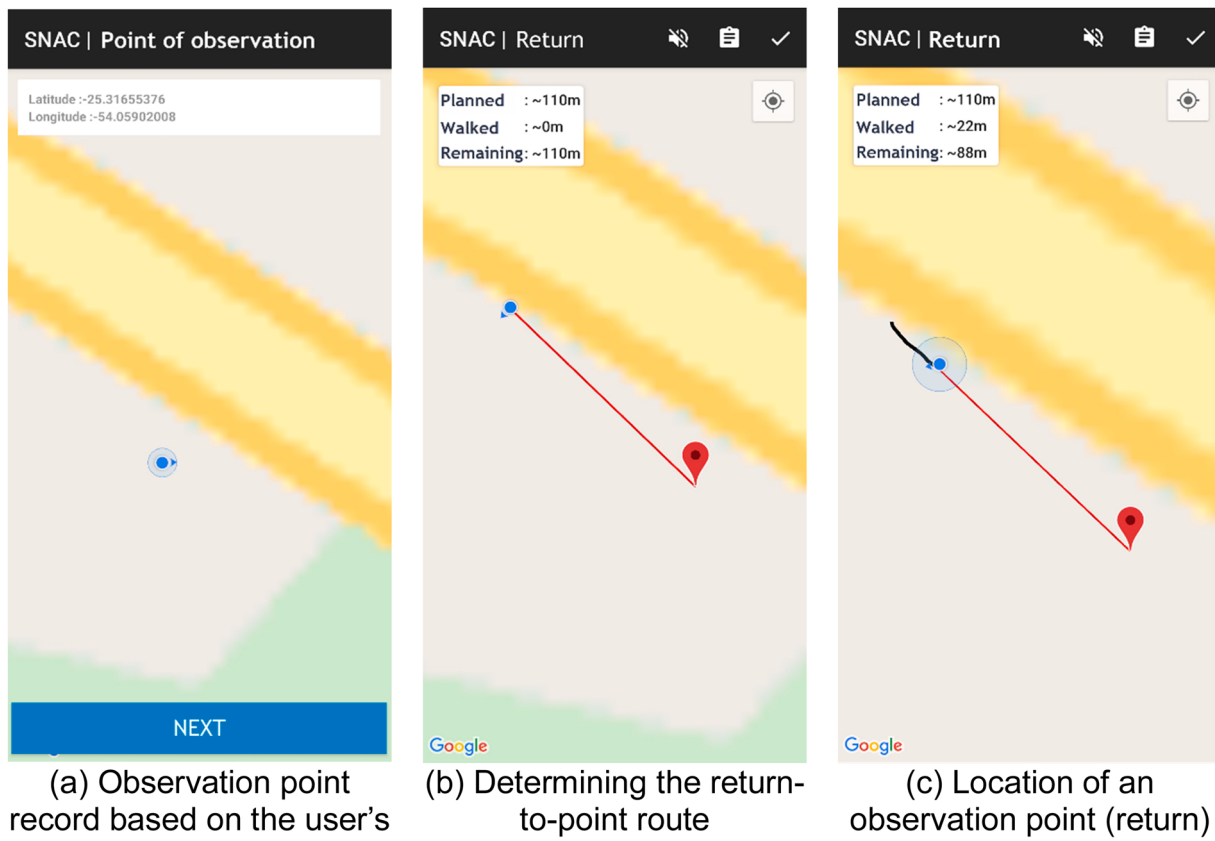


Fig. 9. Module for recording and navigating to an observation point.

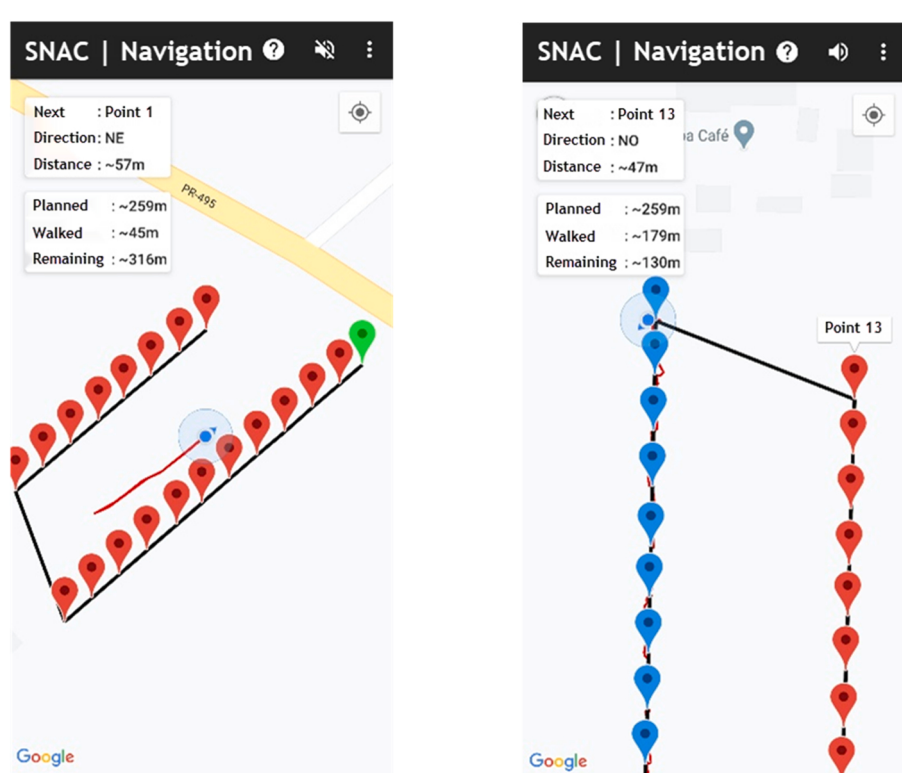
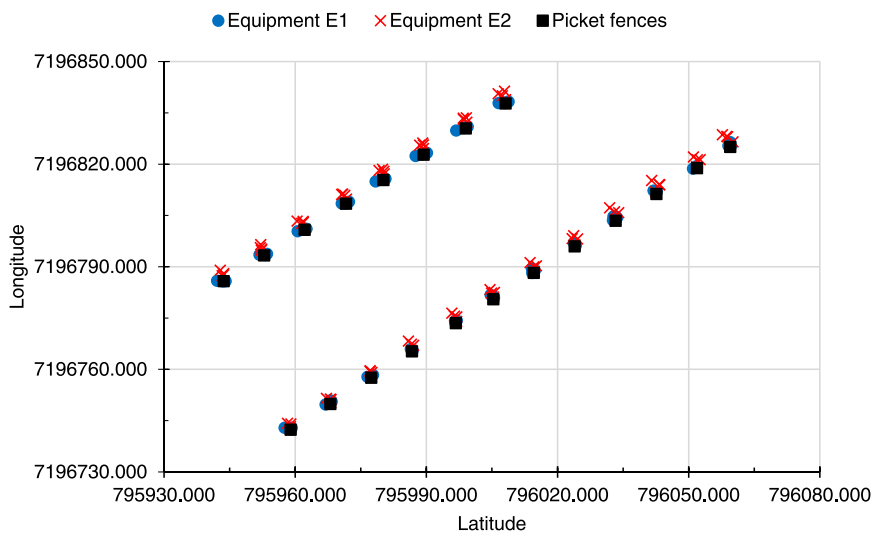


Fig. 10. Navigation module during sampling activities.



**Fig. 11.** Dispersion of equipment positions in relation to picket fences' location using the Universal Transverse Mercator coordinate system.

**Fig. 10b** shows that the user is walking towards point 13, approximately 47 m away, to the Northwest. The sampled points have their color changed to blue, whereas the rest remains in red.

### 3.2. Data dispersion

**Fig. 11** shows a graph with the result of the point location test. The georeferenced coordinates in area A, corresponding to the picket fences, are presented with a black square marker, whereas equipment E1 and E2 are presented by blue and red, respectively. According to the graph in **Fig. 11**, during point location, the equipment presented proximity to the pickets. In visual inspection, it is possible to verify a regularity and a certain standardization in the recovery of data in both equipment, making it possible to identify a greater error in the longitude axis for the E2 equipment. Visually, the Equipment E1 (blue) presented lower

dispersion than Equipment E2 (red).

The visual inspection analysis is supported by data from descriptive statistics (**Table 2**). The E1 equipment presents better mean accuracy in the location of points.

According to the data presented in **Table 2**, the mean location error was 0.72 m for E1 and 2.20 m for E2. The median for E1 indicates that 50% of the readings are below 0.59 m (against 2.20 in E2) and the other 50 % up to a maximum value of 2.28 m (against 4.10 m of E2). That is, E1 presents a data distribution concentrated in values close to 0, whereas E2's distribution is more regular, with values distributed between its maximum and minimum.

The values found are confirmed by the graph in **Fig. 12** – presenting the dispersion of all observed points in relation to its reference point. The initial analysis, that is, that the E2 equipment had a greater error in the longitude axis, becomes more evident in this graph; while the E1

**Table 2**

Descriptive statistics for the values obtained by the RTK station with navigation of equipment's E1 and E2.

	Mean (m)	Standard error (m)	Median (m)	Standard deviation (m)	Variance	Kurtosis	Asymmetry	Min (m)	Max (m)
E1	0.72	0.05	0.59	0.45	0.20	1.32	1.25	0.13	2.28
E2	2.20	0.11	2.20	0.97	0.94	-0.49	-0.34	0.20	4.10

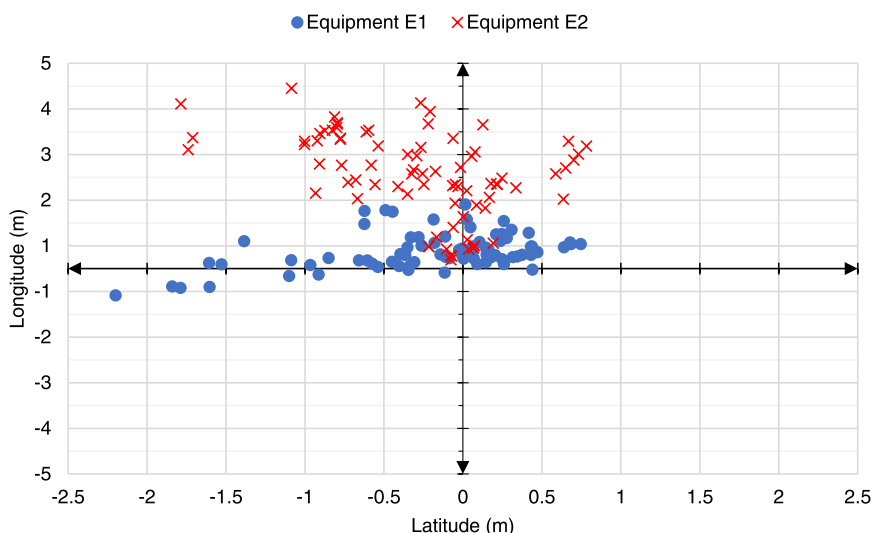


**Fig. 12.** Dispersion of the observed points in relation to the reference point.

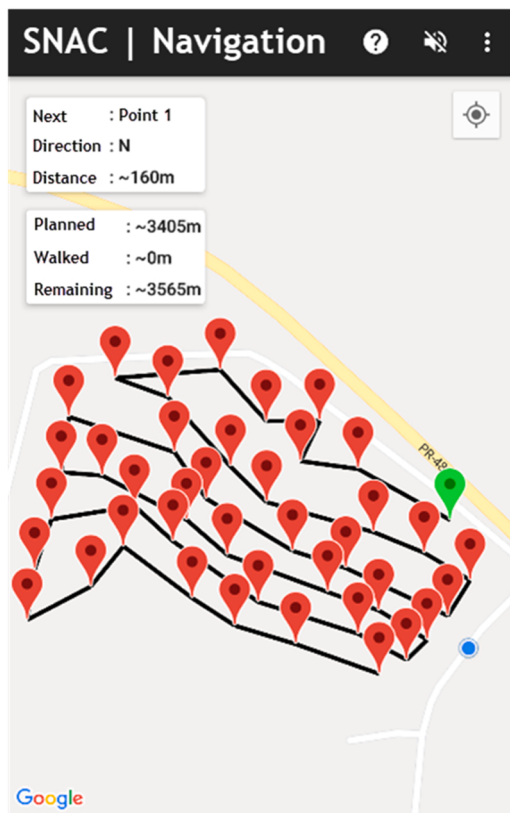


**Fig. 13.** Screen capture of the system with standard route generation for area B.

equipment has a smaller error. The values for latitude are presented close in both pieces of equipment. The difference in the reading of the longitude coordinates between E1 and E2 is possibly the cause of the

difference between the mean values for accuracy in the location of the points.

Based on the tests and on the values obtained, the app (as evaluated running on equipment E1) presents a location similar to that of a commercial GNSS device, being, however, more accurate and precise (according to the standard deviation values). Although the values found show superior precision and accuracy in E1, more field tests (with alternating locations and conditions) are necessary to confirm the difference observed in accuracy. Moreover, a hypothesis test can be established to verify if they differ statistically regarding the accuracy in point location. The mean values indicate that both equipment can be used in most PA applications without a critical accuracy [11].

The values found for E2 are consistent with the manufacturer's specifications and the literature findings, as described in [44] and [49], with accuracy between 2 to 5 m. In the evaluation of a device, [50] concluded that its application shows metric problems. [45] obtained higher accuracy, from 0.5 to 1 m, using a PathFinder ProXT module. Data post-processing, according to the manufacturer and [44], would increase the accuracy to between 1 to 3 m; however, [49] found no statistical difference in accuracy with pre- and post-processed data.

Equipment E1 showed better-quality data than those in the literature. A study by [51] evaluating a smartphone and the Juno receiver found 3.3 m estimated positional error for the smartphone and 5.9 m for Juno, whereas the residual mean error was 1.04 m and 3 m, respectively.

However, this type of study remains incipient, since many studies evaluate accuracy in urban environments, as described by [52], with 7 to 8 m as the mean accuracy, values lower than those found by [53], from 7 to 13 m. This lack of information is corroborated by the systematic review conducted by [16], who emphasizes the significance of mobile devices without mentioning the accuracy of such devices.

### 3.3. Routes

Area B was used in the generation of walking routes based on the existing sampling points. The default route, Fig. 13, corresponds to the

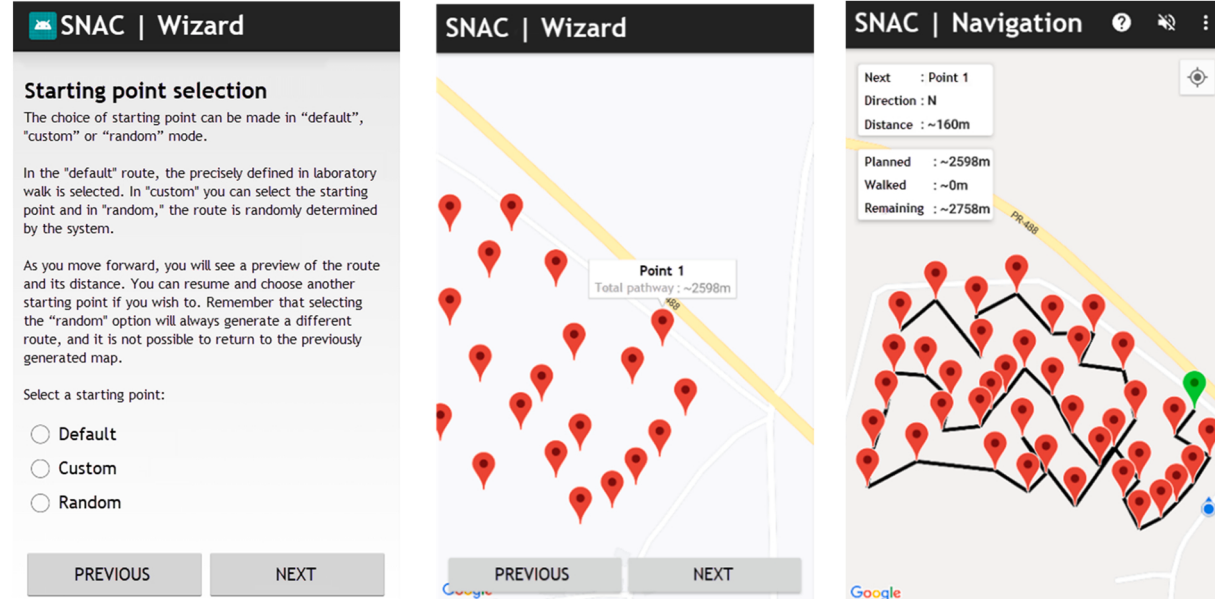


**Fig. 14.** System screenshots related to path generation with a customized starting point.

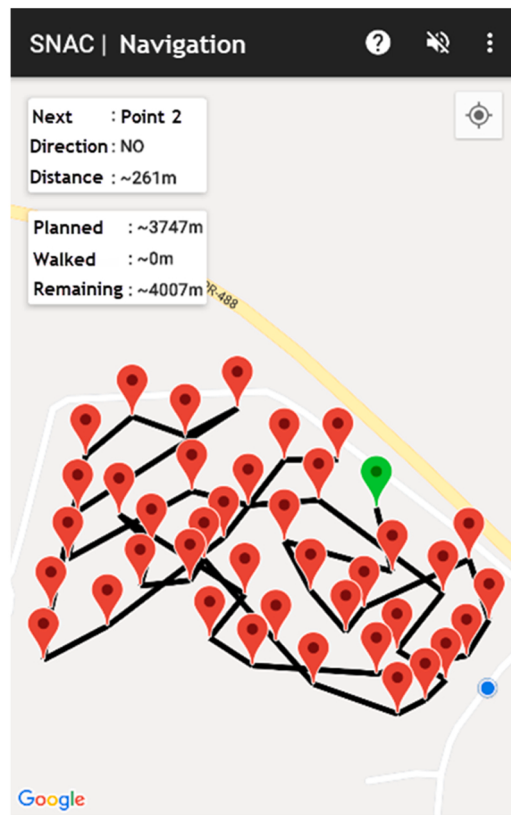


**Fig. 15.** System screenshot to illustrate the path generation by the SA algorithm starting with point 2.

path generated based on the order in which the points are in the file.

The path generated (Fig. 13) comprises a total of 3405 m to be traveled for sampling all points. The first sampling point, corresponding to Point 1, is placed at 160 m from the user's current location at the time the map was generated and can be distinguished from the others by being highlighted in green. The user's position is represented by a blue circle in the lower right corner of the image. This color scheme and representation of the start point is standardized and is not algorithm-dependent. As there was no displacement (Walked = ~0 m), no lines were drawn.

**Table 3**

Comparison between values of each pathway segment using the P, SA, and G algorithms, considering Point 1 as the starting point.

Algorithm	Mean	Dev. Standard	Q1	Median	Q3	Maximum	Minimum	Total
P	87	30.7	65	70	119	140	35	3405
SA	75	33.1	54	69	85	200	31	2948
G	67	29.0	51	63	72	169	31	2598

**Table 4**

Descriptive statistics for G and SA algorithm, with customized cooling rate.

Algorithm	N	Mean	Standard Dev.	Mean SE
G	40.0	2802.7	132.5	20.9
SA (CR=default=0.003)	40.0	3324.2	215.4	34.1
SA (CR=0.0015)	40.0	3042.5	157.8	24.9
SA (CR=0.00075)	40.0	2845.7	132.5	20.9
SA (CR=0.000375)	40.0	2724.6	107.7	17.0
SA (CR=0.0001875)	40.0	2673.8	86.8	13.7
SA (CR=0.00009375)	40.0	2606.3	98.0	15.5
SA (CR=0.000046875)	40.0	2551.8	65.3	10.3

The path definition, as default starting point, custom or random, is defined by the interface showed in Fig. 14a. If the user chooses the custom starting point setting, a selection screen is shown as in Fig. 14b, in which the user must select a point and mark it as the starting point. A caption below the point name already shows the total route size based on the selection.

Fig. 14b shows the map in which Point 1 was selected as a starting point, with 2598 m in total path. By advancing and confirming this information, the user accesses the browser shown in Fig. 14c with the necessary information: next point (01), direction (N) and distance from the user's current location.

The generation of random paths using the SA algorithm does not require user interaction, since it determines the starting and ending points automatically. In the interface shown in Fig. 14a, the option ‘random’ should be selected and a solution is presented, as in Fig. 15, and Point 2 is determined by the algorithm as the beginning of the path.

The paths produced by the P, G, and SA algorithms were evaluated considering Point 1 as the starting point (Table 3). The G algorithm presented the shortest path, 807 m less than the standard walk and 350 m less than an execution of SA algorithm (with default values for cooling rate). The distance of each segment is also lower in the G algorithm.

The mean values indicate approximately 20 m in difference in the distance of each segment, considering P and G paths. The analysis of quartiles also indicates this reduction, and a more expressive difference is observed in Q3, with a 47 m difference. The smaller standard deviation for the G algorithm indicates a higher regularity in the size of each segment.

The SA algorithm had the cooling rate customized, reducing the value by half with each run. The default run and six custom runs were performed for each starting point. The mean of 40 routes was estimated and these values were presented with the values of G in Table 4.

“Mean” corresponds to an estimate of the average population difference. The standard deviation reduces as the CR value decreases, showing that values are getting closer and closer to the mean. The standard error of the mean (SE) estimates the variability among the mean sample if repeated samples from the same population were extracted.

According to Table 4, the G algorithm is numerically superior in the first three SA runs. From the fourth run on, SA presents better values.

Fig. 16 shows a graph with the behavior of the mean 40 paths for each CR value. A decrease in distance is observed as the CR value is reduced.

The red line corresponds to the runtime for one route determination,

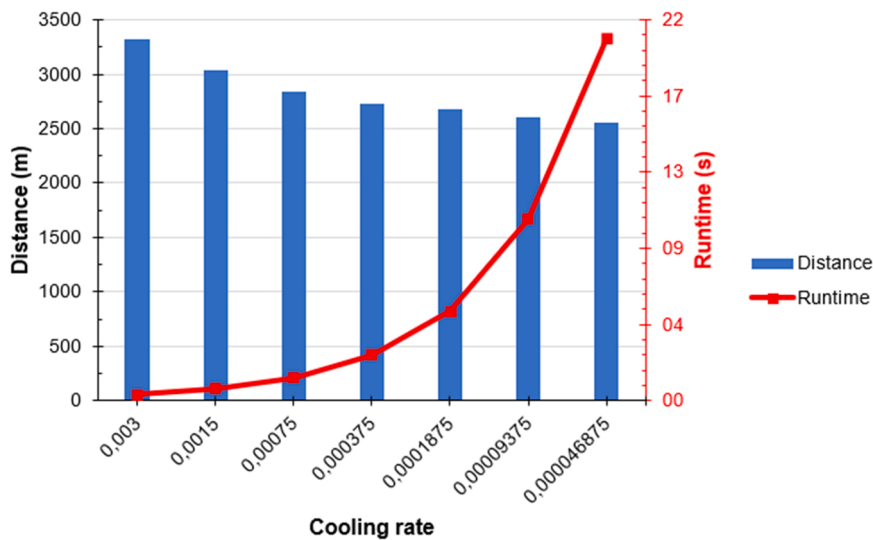


**Fig. 16.** Evolution of the path mean and the time required to determine 1 path, with customized CR value.

**Table 5**

Estimation of the paired difference obtained with the T-test comparing the G algorithm with the SA variations.

	Mean	Standard Deviation	Mean SE	CI	T-value	P-value
SA (CR=default=0.003)	- 521.5	277.5	43.9	(-610.2; -432.7)	- 11.890	0.000
SA (CR=0.0015)	- 239.8	196.7	31.1	(-302.7; -176.8)	- 7.710	0.000
SA (CR=0.00075)	43.0	184.8	29.2	(-102.1; 16.1)	- 1.470	0.149
SA (CR=0.000375)	78.2	187.9	29.7	(18.1; 138.3)	2.630	0.012
SA (CR=0.0001875)	129.0	181.0	28.6	(71.1; 186.9)	4.510	0.000
SA (CR=0.00009375)	196.4	170.0	26.9	(142.1; 250.8)	7.310	0.000
SA (CR=0.000046875)	250.9	146.2	23.1	(204.1; 297.7)	10.850	0.000

which is less than one second at the default CR value and approximately 20 s for the last CR value presented. In the latter scenario, approximately 13 min were spent in determining the 40 routes.

The runtime and determination of each path using the G algorithm was less than one second for all starting points.

The data were subjected to the paired T-test to verify if the means are statistically different (Table 5). Each row of the table corresponds to a mean test between the G algorithm and the specified SA variation, observing the difference between the means ("Mean"), the standard deviation ("Standard deviation") and the standard error of the mean ("Mean SE"). The confidence interval (CI) comprises the interval in which the possible mean differences of the population are inserted, at the chosen level of significance. The T-value is used to estimate the p-value, used as a criterion for rejection or not of the equality hypothesis.

The p-value resulting from the tests in Table 5 does not allow rejecting the hypothesis of equality when CR is equal to 0.00075 or 0.000375, since it was not significant in these two situations. In the other executions, the p-value was significant, and the means can be considered as different. For the default value (0.003) or for the first customization (0.0015), the numerical superiority of the G algorithm is statistically confirmed. There is an equality between means for the second and third customization.

From the fourth customization – with 0.0001875 cooling rate –, the SA algorithm now presents difference and superiority compared to the G algorithm. The runtime for this CR value is approximately four seconds, perfectly acceptable for running on a smartphone or tablet. This execution may require a longer time in devices with lower processing capacity, so we chose to use this value in the algorithm to the detriment of the values in which better mean values of path were obtained.

For the defined CR value, the best path was obtained starting at point

40 with an approximate distance of 2511 m. This path is about 894 m shorter than the default route. An XML file was created containing the duly ordered points, as identified by the SA algorithm to elaborate the path in the app (Fig. 17).

The G algorithm presented interesting path solutions, with a balanced relation between distance and runtime. Therefore, the user should consider this algorithm, given its simplicity and possibility of selecting the starting point, unlike the SA algorithm, which can present start suggestions, but located in the center of the field rather than near to the border, by randomly determining the starting point. The user can accept or reject such suggestion, being able to rerun the algorithm to obtain a new route. This definition should consider the user's location when determining the route, the type of activity, the equipment required, and the means of locomotion available, among other factors.

The determination of paths in sampling routes could consider field elevation, determining the path from a higher to a lower location; however, this is a subjective estimation by choosing the point as a function of elevation or distance. The availability of some means of locomotion, the existence of crops in advanced stage of development – which hinders the user's locomotion – type of sampling performed and the need to use tools for collection are also elements of this formula. Furthermore, it is impossible to measure irregularities in the ground or the presence of obstacles to plan the route.

Thus, SNAC presents unique features when compared with similar apps found in the literature. The NITROGEN INDEX [21] is the only one with a scientific basis, but it has a specific particularity of use and cannot be used in general sampling activities; SOIL SAMPLER [20] requires internet connection, which may hinder its use in the field; GPS FIELDS AREA MEASURE [18,19] suggests the use of an external antenna to ensure accurate operation, that is, it does not present evidence of its

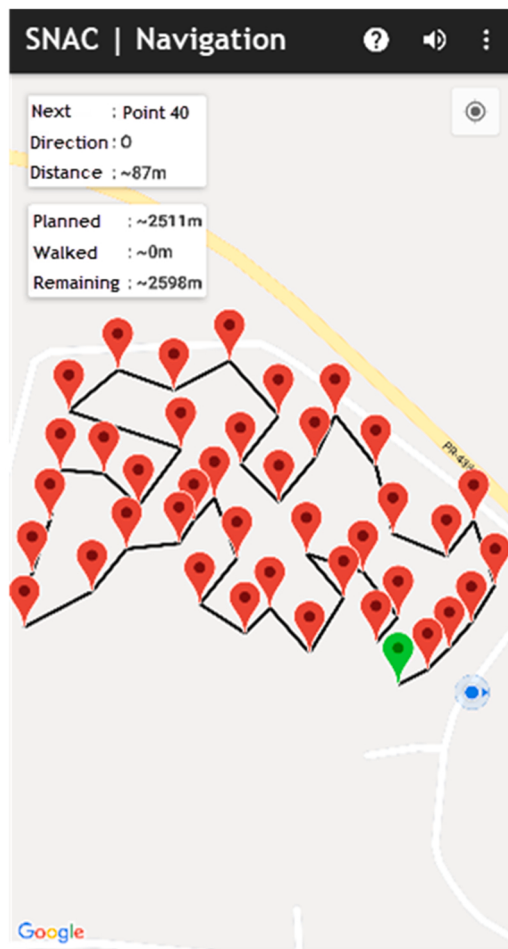


Fig. 17. Best pathway identified by SA algorithm starting at point 40.

consistent operation without such an accessory; AGRI PRECISION [17] demonstrates a greater applicability and sturdiness in sampling activities, but it is not presented in a scientific database, being available in the app store without further specifications. The possibility of user interaction, either by determining the route based on their knowledge, or in the evaluation of which route is the most suitable to the planned activity is also a unique feature of SNAC compared to other existing apps in the market.

#### 4. Conclusion

According to the proposed objective, testing the precision of a smartphone and of a low-cost GNSS device in the location of known sampling points, this study found that the devices tested can be used in PA, especially to work with MZs. Based on the results, the mobile device (E1) showed greater accuracy than the GNSS device E2 (0.72 m against 2.20 m), in addition to greater accuracy (0.45 against 0.97 – based on standard deviation). These results are better than those found by [51] and are in line with the expectation of [23], being a statement of the good accuracy achieved by modern smartphones. This superiority can be partially explained by the multi-constellation capacity of this equipment [54]; however, it still requires further tests to confirm the statistical difference [23].

Thus, given the low cost – both in the acquisition of a smartphone (that can still be used for other agricultural management activities) and in the development of an application – and in view of its similarity with a low cost dedicated GNSS device, its use becomes relevant. This perception corroborates the statement by [55], in which economic aspects and the benefits obtained with PA should be evaluated. Especially

for farmers who have been working with MZs, the presented hardware and software solutions can be used to meet their needs in terms of accuracy. Another element in favor of adoption is that, according to [2], the adoption of PA technologies varies geographically and according to type; that is, it is impossible to establish any rule regarding its use and, for [56], although the PA has several tools, they must be complementary. However, a new evaluation is necessary to consider and generalize the results obtained by any mobile equipment, being possible to confirm the similarity between them, as suggested [23].

Regarding the development of an application designed to assist farmers and service providers in the management of georeferenced sampling points and enable them to guide their location to the field aided by optimized routing techniques based on resources available for mobile devices, the SNAC software has characteristics that are not found in other solutions on the market, found in the systematic review of [16], including the selection of the algorithm for determining the route. The efficiency of the G and SA route determination algorithms is noteworthy, since they have a lower walking value when compared with the route pre-established by the expert. On the other hand, the SA algorithm produces statistically better results than the G algorithm considering the same starting point and the cooling rate customization.

#### Funding

Federal Technological University of Paraná - UTFPR Grant numbers: 25646256b) Conselho Nacional de Desenvolvimento Científico e Tecnológico - CNPq Grant numbers: 309983/2020-7c) Coordenação de Aperfeiçoamento de Pessoal de Nível Superior - CAPES Grant numbers: A1343/2020 P88881.594109/2020-01

#### CRedit authorship contribution statement

**Juliano Rodrigo Lamb:** Conceptualization, Methodology, Software, Writing – original draft preparation, Writing – review & editing. **Everton Coimbra Araújo:** Software, Writing – original draft preparation, Visualization. **Claudio Leones Bazzi:** Conceptualization, Writing – original draft preparation, Validation, Visualization, Supervision. **Márcio Furlan Maggi:** Supervision.

#### Declaration of Competing Interest

The authors declare that they have no known competing financial interests or personal relationships that could have appeared to influence the work reported in this paper.

#### Data Availability

Data will be made available on request.

#### References

- [1] D.J. Mulla, Twenty five years of remote sensing in precision agriculture: Key advances and remaining knowledge gaps (Apr), Biosyst. Eng. vol. 114 (4) (2013) 358–371, <https://doi.org/10.1016/j.biosystemseng.2012.08.009>.
- [2] R. Finger, S.M. Swinton, N. el Benni, and A. Walter, “Precision Farming at the Nexus of Agricultural Production and the Environment,” in ANNUAL REVIEW OF RESOURCE ECONOMICS, VOL 11, vol. 11, no. 1, Rausser, GC and Zilberman, D, Ed. 4139 EL CAMINO WAY, PO BOX 10139, PALO ALTO, CA 94303–0897 USA: ANNUAL REVIEWS, 2019, pp. 313–335. doi: 10.1146/annurev-resource-100518-093929.
- [3] N.M. Thompson, C. Bir, D.A. WIDMAR, J.R. Mintert, Farmer perceptions of precision agriculture technology benefits (Feb), J. Agric. Appl. Econ. vol. 51 (1) (2019) 142–163, <https://doi.org/10.1017/aae.2018.27>.
- [4] R. Kerry, M.A. Oliver, Z.L. Frogbrook, Sampling in precision agriculture. Geostatistical Applications for Precision Agriculture, Springer Netherlands, Dordrecht, 2010, pp. 35–63. doi: 10.1007/978-90-481-9133-8\_2.
- [5] J.P. Molin, T.R. Tavares, Sensor systems for mapping soil fertility attributes: Challenges, advances, and perspectives in brazilian tropical soils (Sep), Eng. Agric. vol. 39 (2019) 126–147, <https://doi.org/10.1590/1809-4430-ENG.AGRIC.V39EP126-147/20190126>.

- [6] P.G. Lawrence, W. Roper, T.F. Morris, K. Guillard, Guiding soil sampling strategies using classical and spatial statistics: a review, *Agron. J.* vol. 112 (1) (2020) 493–510, <https://doi.org/10.1002/agj2.20048>.
- [7] M. Schirrmann, R. Herbst, P. Wagner, R. Gebbers, Area-to-point kriging of soil phosphorus composite samples (Apr), *Commun. Soil Sci. Plant Anal.* vol. 43 (7) (2012) 1024–1041, <https://doi.org/10.1080/00103624.2012.656166>.
- [8] L.P.C. Guedes, M.A. Uribe-Opazo, P.J. Ribeiro Junior, Optimization of sample design sizes and shapes for regionalized variables using simulated annealing (Apr), *Cien. e Invest. Agrar.* vol. 41 (1) (2014) 7–8, <https://doi.org/10.4067/S0718-16202014000100004>.
- [9] Y. Guo, Z. Shi, J. Huang, L. Zhou, Y. Zhou, L. Wang, Characterization of field scale soil variability using remotely and proximally sensed data and response surface method (Mar), *Stoch. Environ. Res. Risk Assess.* vol. 30 (3) (2016) 859–869, <https://doi.org/10.1007/s00477-015-1135-0>.
- [10] M. Keskin, Y.E. Sekerli, S. Kahraman, Performance of two low-cost GPS receivers for ground speed measurement under varying speed conditions (Apr), *Precis. Agric.* vol. 18 (2) (2017) 264–277, <https://doi.org/10.1007/s11119-016-9453-x>.
- [11] S. Rudolph, B.P. Marchant, L. Weihermüller, H. Vereecken, Assessment of the position accuracy of a single-frequency GPS receiver designed for electromagnetic induction surveys (Feb), *Precis. Agric.* vol. 20 (1) (2019) 19–39, <https://doi.org/10.1007/s11119-018-9578-1>.
- [12] T.M. de, A. Silva, G. de, O.G. de, O. Mayrink, D.S.M. Valente, D.M. Queiroz, Integration of a low-cost global navigation satellite system to a single-board computer using Kalman filtering (Jun), *Engenharia Agrícola* vol. 39 (3) (2019) 323–330, <https://doi.org/10.1590/1809-4430-Eng.Agric.v39n3p323-330/2019>.
- [13] U. Deichmann, A. Goyal, D. Mishra, Will digital technologies transform agriculture in developing countries, *Agric. Econ.* vol. 47 (S1) (2016) 21–33, <https://doi.org/10.1111/agec.12300>.
- [14] S. Pongnumkul, P. Chaovatil, N. Surasvadi, Applications of smartphone-based sensors in agriculture: a systematic review of research, *J. Sens.* vol. 2015 (2015) 1–18, <https://doi.org/10.1155/2015/195308>.
- [15] M. Michels, W. Fecke, J.-H. Feil, O. Musshoff, J. Pigisch, S. Krone, Smartphone adoption and use in agriculture: empirical evidence from Germany (Jun), *Precis. Agric.* vol. 21 (2) (2019) 403–425, <https://doi.org/10.1007/s11119-019-09675-5>.
- [16] J. Mendes, et al., Smartphone applications targeting precision agriculture practices—a systematic review (Jun), *Agronomy* vol. 10 (6) (2020) 855, <https://doi.org/10.3390/agronomy10060855>.
- [17] P. Carvalho, As Apps na agricultura, Abolsamia (2017). ([https://issuu.com/abolsamia/docs/abolsamia\\_105/98](https://issuu.com/abolsamia/docs/abolsamia_105/98)) (accessed Aug. 17, 2020).
- [18] A. Buinickaitė, “2,5M farmers are Already Measuring Their Fields for Free,” 2017. (<https://blog.farmis.lt/2-5m-farmers-are-already-measuring-their-fields-for-free-4908bc0ee0a0>) (accessed Aug. 17, 2020).
- [19] A. Randyé, “Why Measuring And Tracking The Field Is So Important?,” 2018. (<https://blog.farmis.lt/why-measuring-and-tracking-the-field-is-so-important-4b949bca2ac8>) (accessed Aug. 17, 2020).
- [20] Farmis, “Soil Sampler (Version 1.0.10—2018).” 2018. [Online]. Available: (<https://play.google.com/store/apps/details?id=com.noframe.farmissoilsamples>).
- [21] J.A. Delgado, K. Kowalski, C. Tebbe, The first Nitrogen Index app for mobile devices: Using portable technology for smart agricultural management (Feb), *Comput. Electron. Agric.* vol. 91 (2013) 121–123, <https://doi.org/10.1016/j.compag.2012.12.008>.
- [22] K. Schenatto, E.G. de Souza, C.L. Bazzi, N.M. Betzek, A. Gavioli, H.M. Beneduzzi, Use of the farmer's experience variable in the generation of management zones (Aug), *Semin.: Ciências Agrar.* vol. 38 (4Supl1) (2017) 2305, <https://doi.org/10.5433/1679-0359.2017v38n4Supl1p2305>.
- [23] P. Dabovic, V. di Pietra, M. Piras, GNSS positioning using mobile devices with the android operating system, *ISPRS Int. J. Geo-Inf.* vol. 9 (4) (2020), <https://doi.org/10.3390/jgi9040220>.
- [24] J. Huuskonen, T. Oksanen, Soil sampling with drones and augmented reality in precision agriculture (Nov), *Comput. Electron. Agric.* vol. 154 (2018) 25–35, <https://doi.org/10.1016/j.compag.2018.08.039>.
- [25] P. Prajapati, The travelling salesman problem (TSP): a case study, *GAP Interdiscip. vol. 875 (2020) 80–83*.
- [26] X. Geng, Z. Chen, W. Yang, D. Shi, K. Zhao, Solving the traveling salesman problem based on an adaptive simulated annealing algorithm with greedy search (Jun), *Appl. Soft Comput. J.* vol. 11 (4) (2011) 3680–3689, <https://doi.org/10.1016/j.asoc.2011.01.039>.
- [27] K. Karabulut, M. Fatih Tasgetiren, A variable iterated greedy algorithm for the traveling salesman problem with time windows (Sep), *Inf. Sci.* vol. 279 (2014) 383–395, <https://doi.org/10.1016/j.ins.2014.03.127>.
- [28] A. Rocha L.B. Dorini Algoritmos gulosos: definições e aplicações *Camp., SP. Camp.* 2004 53.
- [29] V.E. Wilhelm, “O Problema do Caixeiro Viajante,” *sus*, 2020. ([https://docs.ufpr.br/~volmir/PO\\_I\\_12\\_TSP.pdf](https://docs.ufpr.br/~volmir/PO_I_12_TSP.pdf)) (accessed Dec. 26, 2021).
- [30] Dino Cajic, “Greedy Algorithms,” Jun. 05, 2020. (<https://levelup.gitconnected.com/greedy-algorithms-2999d1367828>) (accessed Jan. 18, 2022).
- [31] Y. Eren, İ.B. Küçükdemiral, İ. Üstüoglu, Chapter 2 - Introduction to Optimization, in: R.E.S. Erdinç (Ed.), *O. B. T.-O., Butterworth-Heinemann*, Boston, 2017, pp. 27–74, doi: <https://doi.org/10.1016/B978-0-08-101041-9.00002-8>.
- [32] D. Delahaye, S. Chaimatanan, M. Mongeau, Simulated annealing: from basics to applications, *Int. Ser. Oper. Res. Manag. Sci.* vol. 272 (2019) 1–35, [https://doi.org/10.1007/978-3-319-91086-4\\_1](https://doi.org/10.1007/978-3-319-91086-4_1).
- [33] L. JACOBSON, “Simulated Annealing for beginners,” *The project spot*, 2013. (<http://www.theprojectspot.com/tutorial-post/simulated-annealing-algorithm-for-beginners/6>) (accessed Nov. 11, 2019).
- [34] P.H.C. Camelo, R.L. de Carvalho, Multilayer perceptron optimization through simulated annealing and fast simulated annealing, *Acad. J. Comput. Eng. Appl. Math.* vol. 1 (2) (2020) 28–31, <https://doi.org/10.20873/ajceam.v1i2.9474>.
- [35] M. Lalaoui, A. el Afia, and R. Chihab, “Simulated Annealing with Adaptive Neighborhood using Fuzzy Logic Controller,” in *Proceedings of the International Conference on Learning and Optimization Algorithms: Theory and Applications - LOPAL '18*, 2018, pp. 1–6. doi: 10.1145/3230905.3230963.
- [36] M.H.P. Rodrigues, C.M. dos, S. Machado, M.L.P. de Lima, Simulated annealing aplicado ao problema de alocação de berços, *J. Transp. Lit.* vol. 7 (3) (2013) 117–136, <https://doi.org/10.1590/s2238-10312013000300006>.
- [37] S. Bhardwaj, *Android Operating Systems*, 1st ed., vol. 1, no. 1. 2013.
- [38] J. Gosling, B. Joy, G. Steele, G. Bracha, A. Buckley, *The Java ® Language Specification. Java SE, 8 ed.*, Addison-Wesley, 2014.
- [39] Google Company, “Android Studio Overview | Android Developers,” Google, 2010.
- [40] Google Company, “Google Maps Android API | Google Developers,” Google Developers, 2015.
- [41] N. Lacey, *SQLite. Python by Example*, Cambridge University Press, 2019, pp. 134–146, doi: [10.1017/9781108591942.021](https://doi.org/10.1017/9781108591942.021).
- [42] J.D. Blischak, E.R. Davenport, G. Wilson, A quick introduction to version control with git and github (Jan), *PLoS Comput. Biol.* vol. 12 (1) (2016), e1004668, <https://doi.org/10.1371/journal.pcbi.1004668>.
- [43] E.C. de Araújo, G. Guizzo, J.R. Lamb, and L.J. Merencia, *Padrões de projeto em aplicações WEB*, Florianópolis-SC: Visual Books, 2013.
- [44] N. Aziz, W. Omar, R. Kassim, N. Kamarudin, Remote sensing measurement for detection of bagworm infestation in oil palm plantation (no. June)MPOB Inf. Ser. (MPOB TT No. 502) 2012.(no. June).
- [45] M.M. Kostić, D.Z. Rakić, L.D. Savin, N.M. Dedović, M.D. Simikić, Application of an original soil tillage resistance sensor in spatial prediction of selected soil properties, *Comput. Electron. Agric.* vol. 127 (2016) 615–624, <https://doi.org/10.1016/j.compag.2016.07.027>.
- [46] N.M. Betzek, E.G. de Souza, C.L. Bazzi, K. Schenatto, A. Gavioli, Rectification methods for optimization of management zones, *Comput. Electron. Agric.* vol. 146 (February) (2018) 1–11, <https://doi.org/10.1016/j.compag.2018.01.014>.
- [47] N.M. Betzek, E.G. de Souza, C.L. Bazzi, K. Schenatto, A. Gavioli, P.S.G. Magalhães, Computational routines for the automatic selection of the best parameters used by interpolation methods to create thematic maps, *Comput. Electron. Agric.* vol. 157 (2018) (2019) 49–62, <https://doi.org/10.1016/j.compag.2018.12.004>.
- [48] K. Schenatto, “Utilização de métodos de interpolação e agrupamento para definição de unidades de manejo em agricultura de precisão,” Dissertação, Universidade Estadual do Oeste do Paraná - UNIOESTE, 2014. [Online]. Available: ([http://tede.unioeste.br/tede/tde\\_arquivos/1/TDE-2014-10-07T201706Z-1346/Publico/KelynSchenatto.pdf](http://tede.unioeste.br/tede/tde_arquivos/1/TDE-2014-10-07T201706Z-1346/Publico/KelynSchenatto.pdf)).
- [49] M.F. Fauzi, et al., Tropical forest tree positioning accuracy: a comparison of low cost GNSS-enabled devices, *Int. J. Geoinformatics* vol. 12 (2) (2016) 59–66.
- [50] A. el Abbous, GPS signal accuracy and coverage analysis platform: application to Trimble Juno SB receiver (Jun), *Int. J. Inf. Netw. Secur.* vol. 1 (2) (2012), <https://doi.org/10.11591/ijins.v1i2.532>.
- [51] A. Klimaszewski-Patterson, Smartphones in the field: preliminary study comparing GPS capabilities between a smartphone and dedicated GPS device, *Pap. Appl. Geogr. Conf.* vol. 33 (2010) 270–279.
- [52] S. Clark and E. Levy, “Compared To Specialized Gps Devices, How Good Are Smartphones for Measuring Gps Coordinate Data ?,” pp. 1–8, 2013.
- [53] K. Merry, P. Bettinger, “Smartphone GPS accuracy study in an urban environment,” *PLoS ONE* vol. 14 (7) (2019) 1–19, <https://doi.org/10.1371/journal.pone.0219890>.
- [54] T.G. Lopes, et al., DESEMPENHO OPERACIONAL DE SMARTPHONES EM LEVANTAMENTOS PLANIMÉTRICOS GNSS SOBRE COBERTURAS VEGETAIS DE PASTAGEM E Pinus elliottii ENGELM, Braz. J. Dev. vol. 6 (7) (2020) 53813–53828, <https://doi.org/10.34117/bjdv6n7-867>.
- [55] K. Schenatto, E.G. Souza, C.L. Bazzi, V.A. Bier, N.M. Betzek, A. Gavioli, “Interpolação de dados na definição de unidades de manejo,” *Acta Sci. - Technol.* vol. 38 (1) (2016) 31–34, <https://doi.org/10.4025/actascitechol.v38i1.27745>.
- [56] T.W. Griffin, N.J. Miller, J. Bergtold, A. Shanoyan, A. Sharda, I.A. Ciampitti, “Farm's Sequence of Adoption of Information-intensive Precision Agricultural Technology,” *Appl. Eng. Agric.* vol. 33 (4) (2017) 521–527, <https://doi.org/10.13031/aea.12228>.